



## Research article

# Passive co-treatment of phosphorus-depleted municipal wastewater with acid mine drainage: Towards sustainable wastewater management systems

V. Masindi<sup>a,b,\*</sup>, A. Shabalala<sup>c</sup>, S. Foteinis<sup>d</sup>

<sup>a</sup> Magalies Water, Scientific Services, Research & Development Division, Erf 3475, Stoffberg Street, Brits, 0250, United Kingdom

<sup>b</sup> Department of Environmental Sciences, College of Agriculture and Environmental Sciences, University of South Africa (UNISA), P. O. Box 392, Florida, 1710, South Africa

<sup>c</sup> School of Biology and Environmental Sciences, University of Mpumalanga, Mbombela, Mpumalanga, 1200, South Africa

<sup>d</sup> Research Centre for Carbon Solutions, School of Engineering and Physical Sciences, Heriot-Watt University, Edinburgh, EH14 4AS, United Kingdom



## ARTICLE INFO

## Keywords:

Acid rock drainage (ARD)  
Circular economy and zero liquid discharge (ZLD)  
Sustainable wastewater management  
Wastewater beneficiation and valorisation  
Phosphate rock and phosphorus  
Sustainable development goal (SDG) 6

## ABSTRACT

Industrial processes typically produce large wastewater volumes, which, if left untreated, greatly affect receiving ecosystems. However, wastewater treatment can be costly and energy-intensive, with the developing world particularly struggling with wastewater management. As such, simple and cost-effective solutions are urgently required with the passive (no energy or reagents) co-treatment of different wastewater matrices holding great promise. Here, wastewater from a phosphorus recovery system (chemical precipitation) was co-treated with acid mine drainage (AMD). Specifically, phosphorus-rich municipal wastewater was treated with hydrated lime, as to synthesize a wastewater-derived phosphorus product, i.e., calcium phosphate ( $\text{Ca}_3(\text{PO}_4)_2$ ), also producing a phosphorus-depleted alkaline effluent. The feasibility of valorising this effluent is examined here by using it for the passive co-treatment of real AMD. Different liquid-to-liquid (v/v) ratios were considered, with the optimum ratio (AMD to phosphate-depleted wastewater) being 1:9. The pH of the co-treated effluent was adjusted to 8.4 (from an initial value of 11.5 in the phosphorus-depleted wastewater and 2.2 in AMD), while metals (~100% reduction of Fe, Mn, Ni, Cu, Pb,  $\geq 99.5$  for Al, Zn, and Mg, 80% for Cr, and 75% for As) and sulphate (89.26% reduction) contained in AMD were greatly removed. This was also the case for the remaining orthophosphate that was contained in the phosphorus-depleted wastewater (93.75% reduction). The electrical conductivity was also reduced in both the AMD (88.75%) and the phosphorus-depleted wastewater (69.21%), suggesting the removal of contaminants from both matrices. Results were underpinned by state-of-the-art analytical techniques, including FE-SEM/FIB/EDX, FTIR, and XRD, along with geochemical modelling (PHREEQC). Contaminants were removed through complexation, (co)adsorption, crystallization, and (co)precipitation. Overall, results suggest that the co-treatment of these wastewater matrices is feasible and could be directly scaled up (e.g., using waste stabilization ponds), while opportunities for the beneficiation of the produced sludge and for water reclamation (e.g., through membrane filtration) could also arise, further promoting the sustainability of this passive co-treatment method.

## 1. Introduction

Phosphorus (P) is an essential mineral and an important resource that is consumed in vast quantities in agriculture. This has resulted in increased mining and depletion of phosphate rock, which typically contains calcium phosphate ( $\text{Ca}_3(\text{PO}_4)_2$ ), the main source for P fertilizer production (Rittmann et al., 2011). As a result, alternative sources for the sustainable mining/recovery of P have been recently sought, with

municipal wastewater (MWW) having emerged as a promising source for the recovery of low-grade phosphate (Egle et al., 2016). The recovery of P from MWW can also improve the quality of the treated effluent (Masindi and Foteinis, 2021; Masindi et al., 2022a) and thus, in theory, could reduce the cost, energy, and environmental footprint of wastewater management. It will also safeguard human health and the environment, since the release of untreated MWW, a common practice in the developing world, greatly affects receiving water bodies leading, among

\* Corresponding author. Department of Environmental Sciences, College of Agriculture and Environmental Sciences, University of South Africa (UNISA), P. O. Box 392, Florida, 1710, South Africa.

E-mail addresses: [vhahangwelem@magalieswater.co.za](mailto:vhahangwelem@magalieswater.co.za) (V. Masindi), [s.foteinis@hw.ac.uk](mailto:s.foteinis@hw.ac.uk) (S. Foteinis).

<https://doi.org/10.1016/j.jenvman.2022.116399>

Received 23 July 2022; Received in revised form 14 September 2022; Accepted 26 September 2022

Available online 6 October 2022

0301-4797/© 2022 Elsevier Ltd. All rights reserved.

others, to their eutrophication (Masindi and Foteinis, 2021). As such, if this element (P) is recovered (mined) from MWW, this could lead to reduced ecological and environmental stresses, while its valorisation (e.g., for P fertilizer production) could credit the system with avoided cost and environmental impacts and possibly even make this MWW management practice self-sustainable (Mavhungu et al., 2020). Finally, this MWW management practice could address, at least partly, the problem of phosphate rock over-exploitation and depletion (Mavhungu et al., 2020; Masindi and Foteinis, 2021).

On the other hand, acid mine drainage (AMD) or acid rock drainage (ARD) is a wastewater effluent that is typically formed through the oxidation of sulphide bearing minerals (e.g., pyrite and arsenopyrite) (Amos et al., 2015; Shabalala et al., 2017; Masindi et al., 2018a). It comprises elevated levels of metals and heavy metals (e.g., Cu, Zn, Ni, Cr, As, and Pb), metalloids, oxyanions, rare earth metals, and radionuclides (Nordstrom et al., 2015). This wastewater effluent mainly traces back to coal and gold mining, and it is prevalent in areas with intense mining activities. Chemical species in AMD are known to pose mutagenic, teratogenic, and carcinogenic effects to living organisms (Masindi et al., 2022c). As such, to protect receiving environments and human health strict regulations and discharge limits have been proposed (WHO, 2017). However, due to the complexity and cost of existing treatment processes, developed and primary developing countries struggle with its effective management (Wei et al., 2008; Cheng et al., 2011; Maha, 2022; Masindi et al., 2022b). Although AMD treatment is available in some places and primarily in active mines, this is not typically the case and AMD will decant to adjacent environments greatly imposing on its quality and highlighting the urgent need for its sustainable treatment (Masindi et al., 2022c).

Specifically, several technologies have been proposed for AMD treatment, including filtration (Agboola, 2019), ion exchange (Nleya et al., 2016), adsorption (Simate and Ndlovu, 2014), precipitation (Masindi et al., 2014, 2018c), and bioremediation (Nguegang et al., 2021, 2022). However, these technologies are energy and resource intensive, and particularly the first ones where frequent energy and material inputs, along with operation and maintenance (O&M) are required, i.e., active treatment (Kefeni et al., 2017; Park et al., 2019; Wilfong et al., 2022). For this reason, research has also focused on alternative management approaches (Tony and Lin, 2022a), with the co-treatment of AMD with other wastewater matrices, and notably municipal wastewater (MWW), having emerged as a promising alternative treatment method (Wei et al., 2008; Tony and Lin, 2022b).

Various studies have examined the co-treatment of AMD with MWW (Spellman et al., 2020a), including raw (Strosnider et al., 2011), screened (Hughes and Gray, 2013), secondary (Spellman et al., 2020b), and sludge dewatering MWW (Masindi et al., 2022b). However, in these cases, the P that is contained in MWW cannot practically be recovered, since it (co)precipitates along with the metals and minerals contained in AMD and forms a highly heterogeneous sludge. As such, here, wastewater from a phosphorus recovery system was used, for the first time, for the passive treatment, i.e., no energy or reagents are consumed, of high-strength AMD. Specifically, in the previous works of our group phosphate recovery from MWW was accomplished through chemical precipitation, and then successfully employed for the synthesis of  $\text{Ca}_3(\text{PO}_4)_2$  (Masindi and Foteinis, 2021). Interestingly, the effluent of this process was found to be rich in calcium (Ca) and highly alkaline, which suggests that it could be used for AMD neutralisation and, most likely, due to its elevated Ca content for gypsum synthesis since AMD is rich in sulphate (Masindi et al., 2018b).

Therefore, this study seeks to evaluate, for the first time, the feasibility of passively co-treating the MWW effluent/supernatant from the  $\text{Ca}_3(\text{PO}_4)_2$  synthesis process with real high-strength AMD, focusing on the fate and partitioning of inorganic chemical species that are contained in both wastewater matrices. As such, this study expands the body of knowledge not only on the use of different MWW matrices for AMD passive co-treatment (i.e., phosphorus-depleted MWW instead of raw

**Table 1**

Examined L-L ratios for the passive co-treatment of AMD and CPW. Conditions: 12 h contact time (passive mixing), ambient temperature and pH. Experiments were performed in triplicate and results are reported as mean values.

Number	AMD:CPW ratio (mL: mL)	Initial pH values (AMD: CPW)	Final pH value
1	10:50	pH 2.2:11.5	4.18
2	10:60	pH 2.2:11.5	5.58
3	10:70	pH 2.2:11.5	6.69
4	10:80	pH 2.2:11.5	8.16
5	10:90	pH 2.2:11.5	8.39

(Strosnider et al., 2011), screened (Hughes and Gray, 2013), or secondary MWW (Spellman et al., 2020b)) but also on the passive treatment process itself (i.e., one-stage passive mixing instead of three- (Strosnider et al., 2013a) or four-stage batch reactor passive mixing (Strosnider et al., 2011) or instead of passive mixing inside pipes (Spellman et al., 2020b)). Furthermore, the proposed passive co-treatment process can open up new avenues and opportunities for using wastewater from P recovery streams, which, given the dwindling phosphate rock resources, are on the rise (Egle et al., 2016). Finally, this sustainable wastewater management paradigm can further promote circular economy schemes and promote the United Nations (UN) Sustainable Development Goals (SDGs) and particularly SDG 6 which deals with the availability of water and its sustainable management.

## 2. Materials and methods

### 2.1. Sample collection

The phosphorus-depleted wastewater, calcium phosphate wastewater (CPW) thereafter, was collected from a  $\text{Ca}_3(\text{PO}_4)_2$  recovery system, which was examined in previous works of our group (Masindi and Foteinis, 2021). Immediately after collection it was passed through a Macherey-Nagel filter paper (MN 615. Ø125mm) to remove suspended solids and debris. Then, it was stored in high-density polyethylene (HDPE) containers, until utilisation for the co-treatment experiments. The high-strength AMD was collected from a storage dam, where AMD seeps through the toe of a large coal mine tailings pile and is concentrated into an evaporation pond, in an active coal mine in Mpumalanga province, South Africa. As such, the AMD was highly concentrated, due to evaporation, and fully oxidised since it is exposed to air (atmospheric oxidation). The collected AMD was also passed through Macherey-Nagel filter papers (MN 615. Ø125mm) to remove suspended solids and debris and then stored in HDPE containers until utilised for the co-treatment experiments. Standard methods and procedures for sample handling were duly considered.

### 2.2. Aqueous samples characterization

The following analytical techniques were used for the characterization of the collected aqueous matrices (AMD and CPW), as well as of the effluent that was generated after their passive co-treatment. Specifically, the pH and electrical conductivity (EC) were directly measured by means of a multi-parameter probe (HANNA instrument, HI9828). Minerals were quantified using the Thermo Scientific™ Gallery™ Plus Discrete Analyser, which also performs photometric (colorimetric and enzymatic) and electrochemical (pH and EC) analyses. Finally, inductively coupled optical emission spectroscopy (ICP-OES) (Agilent 5110 Synchronous Vertical Dual View (SVDV)) was used to identify the chemical compositions of CPW and AMD, as well as of the CPW-AMD co-treated effluent. Measurements were performed in an ISO/IEC 17025:2017 accredited laboratory in South Africa.

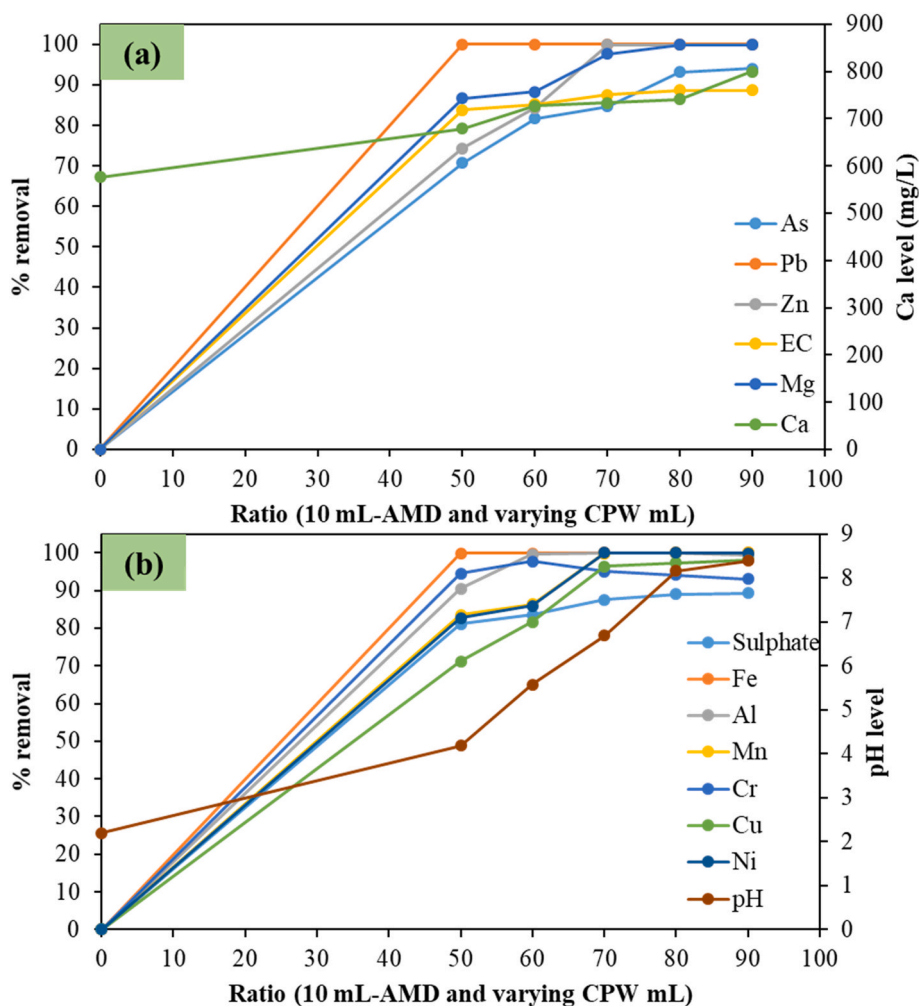


Fig. 1. Variations in the levels and percentage removals of different water quality determinants, i.e., (a) EC, Ca, Mg, Zn, Pb, and As; and (b) Fe, Al, Mn, Cu, Cr, Ni, sulphate, and pH with varying AMD-CPW ratios (conditions: 10 mL AMD, ambient temperature and pH, and passive mixing for 12 h).

### 2.3. Co-treatment assays

To determine the effect of liquid-to-liquid (L-L) ratio that optimizes the treatment efficacy of both effluents, and particularly AMD which is highly concentrated, different L-L ratios (AMD:CPW) were examined, ranging from as low as 1:9 to as high as 1:5 (Table 1). In detail, experiments were carried out at bench scale, whereby the volume of AMD was kept constant at 10 mL and different dosages of CPW, i.e., 50, 60, 70, 80, and 90 mL were added and left to react, leading to contaminants removal. To make the treatment system cost-effective and versatile, particularly for the developing world context where capital and resources are scarce, passive mixing was considered. Therefore, neither the temperature nor the pH of the effluents were controlled/manipulated, but more importantly passive mixing (i.e., no energy or resources/reagents are consumed) was considered as the means of promoting the chemical reactions between the different contaminants that were harboured in each wastewater matrix. To this end, the different L-L ratios were left for 12 h, which is ample time for the wastewater matrices passively react (passive mixing) and equilibrate.

### 2.4. Characterization of the product sludge

To identify the fate of the contaminants, post their passive co-treatment, apart from the co-treated effluent (supernatant) the sludge that was generated (product sludge thereafter) was also characterized. To this end, state-of-the-art analytical techniques were employed to

identify the elemental, mineralogical, microstructural, and functional properties of the product sludge. These include a high-resolution field emission-scanning electron microscope (FE-SEM), equipped with the cobra column focused ion beam (FIB) and energy-dispersive X-ray spectroscopy (EDX), i.e., the Carl Zeiss AURIGA® Series modular Cross-Beam® workstation, as well as Fourier transform infrared spectroscopy (FTIR) equipped with attenuated total reflectance (ATR), i.e., the PerkinElmer Spectrum 100. An X-ray fluorescence (XRF) spectrometer was also used to identify the elemental composition, i.e., the Thermo Scientific™ ARL™ PERFORM™ X instrument along with the UniQuant™ software for standardless XRF analysis. To improve accuracy, borate fusion, using lithium tetraborate as the flux, was employed, while to determine the loss on ignition (LOI) the product sludge was roasted in an alumina refractory crucible. Finally, X-ray diffraction (XRD) was also employed, i.e., the PANalytical X'Pert Pro powder diffractometer in  $\theta$ - $\theta$  configuration, with an X'Celerator detector, and variable divergence- and fixed receiving slits with Fe filtered Co-K $\alpha$  radiation ( $\lambda = 1.789 \text{ \AA}$ ). For the XRD analyses the samples were prepared according to the standardized Panalytical back loading system, which provides nearly random distribution of the particles, while the mineralogy was determined by selecting the best-fitting pattern, from the Inorganic Crystal Structure Database (ICSD) database, to the measured diffraction pattern using X'Pert HighScore Plus software. The relative phase amounts (wt% of crystalline portion) were estimated using the Rietveld method.

**Table 2**

Results on the passive co-treatment of real AMD and CPW at a 1:9 ratio, 12 h contact time, and ambient temperature and pH.

Element	AMD (ppm)	CPW (ppm)	Product water (ppm)
Sulphate	17255.0	17.0	1853.0
Iron (Fe)	4300.0	0	0
Aluminium (Al)	740.0	0.2	3.6
Manganese (Mn)	140.0	0	0
Chromium (Cr)	0.10	0.01	0.01
Copper (Cu)	0.20	0.01	0
Nickel (Ni)	1.77	0	0
Arsenic (As)	0.04	0.01	0.01
Lead (Pb)	0.25	0	0
pH @ 25 °C	2.2	12.1	8.4
Electrical Conductivity @ 25 °C	2719.0	994.0	306.0
Zinc (Zn)	14.0	0.02	0.02
Orthophosphate	0.03	0.16	0.01
Calcium (Ca)	576.0	835.0	400.0
Magnesium (Mg)	771.0	0.03	0.68

### 2.5. Prediction of the synthesized mineral phases

To calculate the distribution of aqueous species (speciation) and predict the chemical species and/or minerals that are more likely to be synthesized and precipitate from the passive interaction of AMD with CPW, the PHREEQC geochemical model was employed making use of the wateq4f.dat, phreeqc.dat, minteq.V4.dat, and minteq.dat databases (Masindi, 2016). PHREEQC was primarily used as a tool to complement the experimental results. To this end, the saturation indices (SIs) of the mineral phases, based on solution compositions and their respective concentrations, were estimated and used as indicators for the precipitation (supersaturated solution). In PHREEQC, SI values lower than zero (i.e., the omega ( $\Omega$ ) value is lower than unity (1)) denote an unsaturated solution, SI values equal to zero ( $\Omega = 1$ ) denote a saturated solution and, lastly, SI values higher than zero ( $\Omega > 1$ ) denote a super-saturated solution and thus a highly likelihood of precipitation.

## 3. Results and discussion

### 3.1. Effect of liquid-to-liquid ratio

As mentioned above, a wide range of L-L ratios (AMD:CPW), in the range 10:90 to 10:50 mL:mL, were examined (Table 1) and results are shown in Fig. 1.

As shown in Fig. 1, there is an increase in the percentage removal of the inorganic contaminants under study with a decrease in the AMD:CPW ratio, i.e., with increasing CPW volume. This is also suggested by the reduction in EC with increasing CPW volumes, which is attributed to the removal of chemical species from the aqueous system (Fig. 1a). Only the Ca levels and pH were observed to increase with an increase in CPW volume, i.e., with decreasing L-L ratios, however, in both cases this was beneficial for the co-treatment process. Specifically, the enrichment of the co-treated effluent with Ca, which is contained in CPW (Fig. 1a), will lead to the removal of sulphate that is contained in AMD and its precipitation as gypsum (Fig. 1b). Similarly, the pH was observed to increase with decreasing L-L ratios, but again this is beneficial since AMD's pH was highly acidic (2.2). From the results shown in Fig. 1, at the last examined CPW volume (10:90 ratio) the pH is around 8.4. This signifies the increase of alkalinity in the system, from the increased dosages of CPW, which, among others, will promote the precipitation of metals as metal hydroxides (Park et al., 2019; Ighalo et al., 2022). Overall, the obtained results denote that heavy metals, metalloids, and oxyanions that were contained in AMD were greatly removed with decreasing L-L ratios, with the percentage removals being optimized at the last examined CPW volume and being, from higher to lower score,  $Fe \geq Mn \geq Ni \geq Cu \geq Pb \geq Mg > Zn > Al > Cr > sulphate > As$  (Fig. 1). Therefore, it

appears that the passive co-treatment of CPW and AMD provides an effective solution for the management of both effluents.

It should be noted that the PHREEQC geochemical model (section 3.4) suggested that chemical species existed as divalent, trivalent, and other complexes and predicted that dilution, complexation, crystallization, (co)adsorption, and (co)precipitation are the main mechanisms underlying contaminants removal, as has been also suggested elsewhere for such effluents (Simate and Ndlovu, 2014; Muedi et al., 2021; Masindi et al., 2022b; Shabalala and Masindi, 2022).

### 3.2. Passive co-treatment at optimal conditions

From the results discussed above, it appears that the optimal condition for the treatment of both effluents is the 1:9 (AMD:CPW) ratio, and here the co-treatment efficacy is reported at bench scale (Table 2).

As shown in Table 2, the passive co-treatment of real AMD and CPW greatly reduced the levels of contaminants in both wastewater matrices. In detail, AMD was predominated by Fe and sulphate amongst other chemical species, which are traced back to pyrite oxidation. On the other hand, the CPW was phosphorus-depleted and this is reflected in the low concentration of orthophosphate, but it was rich in Ca and alkalinity, which traces to the dissolution of hydrated lime during P recovery from MWW. After the passive interaction of the two wastewater matrices, at 1:9 AMD to CPW ratio, the pH was around 8.4, from the very low pH in AMD (2.2) and the very high pH in CPW (11.5). This could be attributed to the counteraction of acidity and alkalinity, including the formation of metal hydroxides as acid forming compounds. There was also a significant reduction in EC in both wastewater matrices, and particularly in AMD, which is traced back to the attenuation of chemical species. More importantly, the chemical species (contaminants) from both wastewater matrices were greatly reduced, registering very high percentage removals (Fig. 1 and Table 2) and specifically  $\geq 99.9\%$  removal efficacy was achieved for Fe, Mn, Ni, Cu, and Pb, while Al, Zn, and Mg removal was also very high ( $\geq 99.5\%$ ), followed by, Cr (90%), sulphate (89.3%), and As (75%).

Overall, the passive co-treatment of AMD and CPW appears as a promising intervention, which can lead to the treatment of both wastewater matrices to a great extent. However, the generated co-treated effluent is not fit for release into the environment, primarily due to the relatively high sulphate content, let alone used for water reclamation. As such, a polishing technology (e.g., membrane filtration) could be integrated to remove residual sulphate and possibly lead to water reclamation. Therefore, this co-treatment initiative could synergistically be considered a low-cost and passive treatment method, particularly for mining areas that are near MWW facilities. Nonetheless, it requires a much higher CPW volume compared to the AMD volume. Coupling lime dosing to further attenuate residual sulphate as an integrated step will further attenuate sulphate to the required discharge limit and possibly enable the release of the effluent into the environment. If lime or another softening agent was to be added in the co-treated process, a much lower volume of CPW, compared to the AMD volume, would be also required. The proposed process could be also incorporated in existing industrial treatment processes and particularly in waste stabilization ponds. Finally, apart from being able to reclaim water (e.g., through membrane filtration), the recovery of valuable minerals from the product sludge could also be possible, since, as will be discussed below, large amounts of minerals are embedded in its matrix. The beneficiation of the product sludge could also reduce the cost and possibly the environmental footprint of the process and thus can be another avenue for future research.

### 3.3. Characterization of the minerals contained in product sludge

To complement and corroborate the aforementioned results for the raw (AMD and CPW) and passive co-treated aqueous matrices, the solid material that was formed and precipitated during the AMD-CPW passive

**Table 3**

The elemental composition (wt%) of the product sludge as measured by XRF.

Chemical species	Composition (wt%)	Chemical species	Composition (wt%)
SiO <sub>2</sub>	1.32	MnO	0.77
Al <sub>2</sub> O <sub>3</sub>	6.45	NiO	0.01
MgO	2.39	CuO	<0,01
Na <sub>2</sub> O	0.53	ZrO <sub>2</sub>	<0,01
P <sub>2</sub> O <sub>5</sub>	0.30	S	14.82
Fe <sub>2</sub> O <sub>3</sub>	32.96	Cl	<0,01
K <sub>2</sub> O	0.36	Co <sub>3</sub> O <sub>4</sub>	0.04
CaO	23.95	ZnO	0.08
TiO <sub>2</sub>	<0,01	Ag <sub>2</sub> O	0.08
V <sub>2</sub> O <sub>5</sub>	<0,01	LOI	15.62
Cr <sub>2</sub> O <sub>3</sub>	<0,01	TOTAL	99.93

co-treatment, i.e., the product sludge, was also characterized. Results are presented and discussed below.

### 3.3.1. Elemental composition

The elemental composition (wt%) of the product sludge, was identified and quantified using XRF and results are shown in Table 3.

As shown in Table 3, the product sludge was predominated by elements that were prevalent in AMD, particularly Fe and S (sulphate), and to a lesser extent in CPW, particularly Ca. Furthermore, the relatively high LOI denotes the presence of water, organic matter, and other volatile substances and, most likely, suggests that the product sludge is hydrated. Furthermore, traces of other chemical species such as Al, Si, Mg, Na, P, K, and Mn were identified in the product sludge and these are, by and large, traced back to the AMD matrix. As such, the presence of these chemical species in the product sludge confirms their removal from the raw wastewater matrices, as the PHREEQC estimates also suggested (section 3.4). Furthermore, the presence of Ca and S in the product sludge denotes the possible formation of gypsum, whereas Fe and other metals postulate the formation of metals hydroxides, oxyhydroxides, and other mineral complexes.

### 3.3.2. Elemental properties

The elemental properties of the product sludge were measured by the means of EDX and results are shown in Fig. 2.

Specifically, in Fig. 2 the EDX results are shown, which corroborate what was reported by the XRF technique (section 3.3.1). In detail, the EDX results confirmed the presence of O, Ca, S, and Fe as major elements in the product sludge, along with traces of Al, Cl, Mg, Si, K, and Mn. C was also detected, but, most likely, this traces back to sample coating (fine carbon layers for the SEM measurements) and not to the product sludge itself. The predominance of O and Fe denotes the possible formation of Fe-hydroxide, whilst the presence of Ca and S suggests the

possible formation of gypsum, which is in agreement with the PHREEQC's estimates (section 3.4).

### 3.3.3. Functional and mineralogical properties

The functional and mineralogical properties of the product sludge were measured by the means of FTIR, and XRD, respectively, and the corresponding results are shown in Fig. 3.

The FTIR results are shown in Fig. 3a and these also corroborate the above-mentioned EDX results, as well the XRF results (section 3.3.1). Firstly, the FTIR technique unpacked the presence of Fe-O bending and stretching in the product sludge at 560, 600, 950, and 3500 cm<sup>-1</sup> (Tabelin et al., 2020), which denotes the presence of Fe-based minerals. The sulphate (SO<sub>4</sub>) stretching at 1050 and 1600 cm<sup>-1</sup> (Tabelin et al., 2017) confirms the possible formation of gypsum, while the presence of water (-OH group) denotes that the product sludge is hydrated, and the mineral phases therein are in hydrated form and nature (hydroxides). In

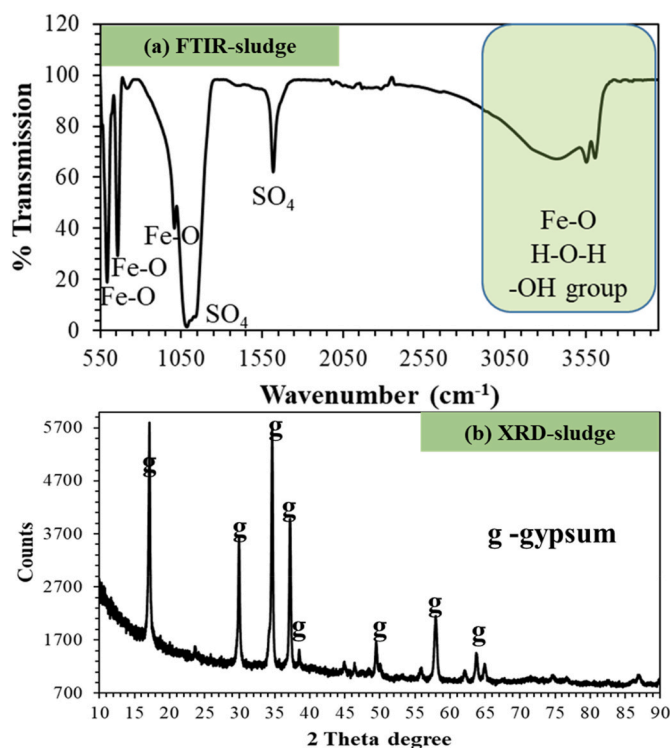


Fig. 3. The a) functional and b) mineralogical properties of the product sludge.

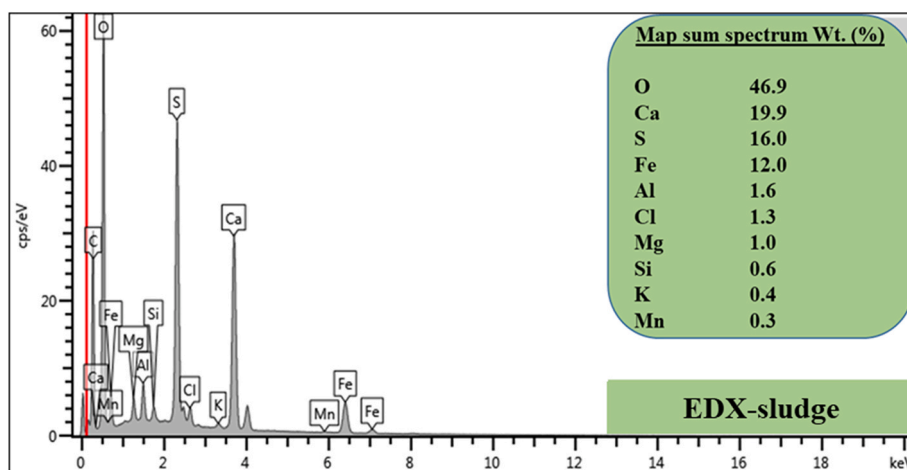


Fig. 2. The elemental properties of the product sludge as measured by EDX.

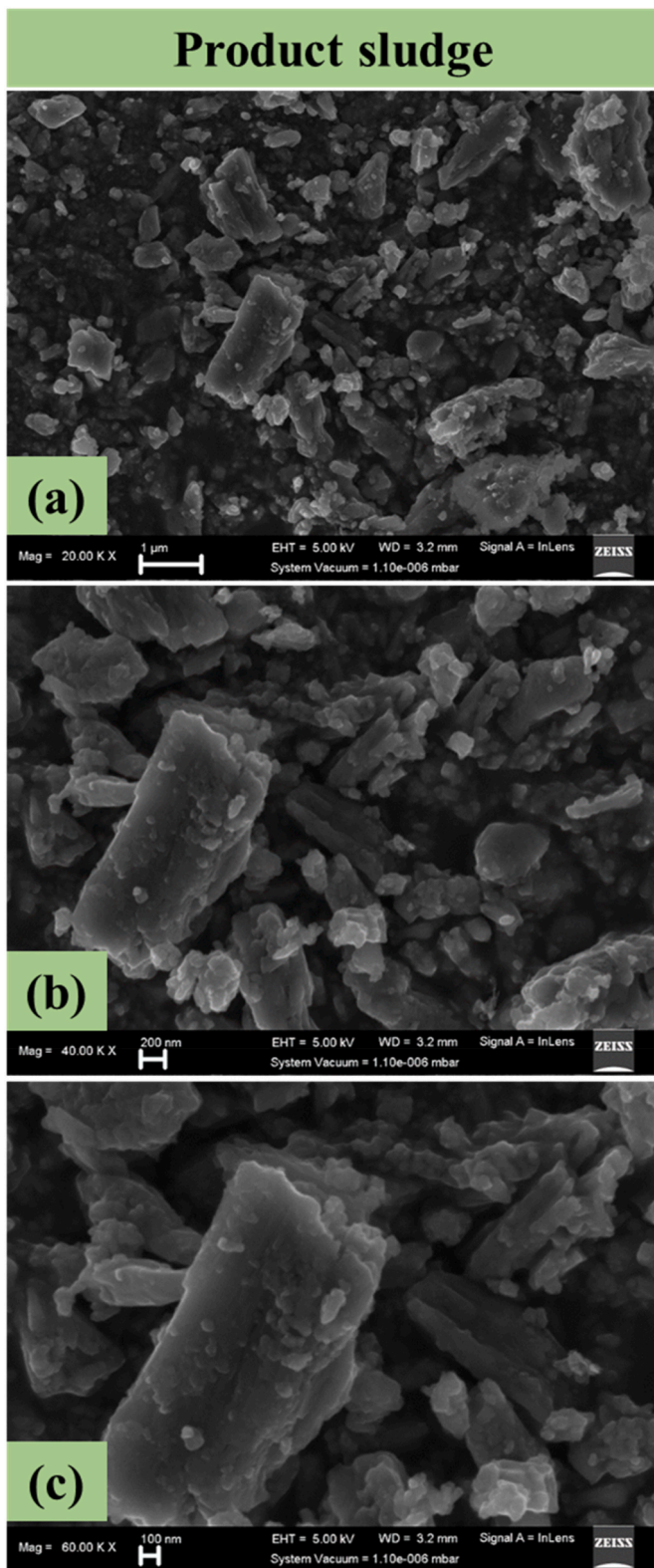


Fig. 4. The high-resolution FE-SEM microstructural image showing the morphological properties of the product sludge from the passive co-treatment of real AMD and CPW at (a) 1 µm, (b) 200 nm, and (c) 100 nm magnification.

Fig. 3b the XRD results are shown, where it is observed that the product sludge comprises calcium sulphate (gypsum) as its main mineral. However, the peaks were observed to be very noisy, hence confirming the presence of amorphous phases which could not be quantified by XRD

technique.

Overall, the obtained results are in agreement with the ones presented in the aqueous characterization section, and further confirm that the product sludge is a sink of the main chemical species contained in both wastewater matrices.

### 3.3.4. Morphological and microstructural properties

The morphological and microstructural properties of the product sludge were identified using FIB-SEM. Vivid and high-resolution images were obtained, clearly showing the fine microstructural and morphological properties of the product sludge (Fig. 4).

As shown in Fig. 4, the product sludge was observed to be heterogeneous in nature, mainly comprising rod-like shaped structures sandwiched with spherical and octagonal-like structures throughout the sludge's surface. Interestingly, the microstructural and morphological properties were observed to remain similar regardless of the employed magnification (from 1 µm to 100 nm), hence suggesting the uniformity and homogeneity in the product sludge. The distinctive and fully crystallized nature of the product sludge further highlights the homogeneity of the embedded minerals.

### 3.3.5. Elemental mapping

In this section, the SEM micrograph and corresponding EDX elemental mapping of the product sludge are reported (Fig. 5). The principal aim was to acquire insight into the elements that comprise the product sludge. Specifically, the elemental mapping confirmed the presence of O, S, Ca, Fe, Al, Mn, Mg, K, and Cl in the product sludge (Fig. 5). These elements correspond to the sum of peaks that were identified in the FE-SEM image (Fig. 4). The presence of rod-like structures, which mainly represents Ca, O, and S, denote the formation of hydrated gypsum (Masindi et al., 2019). The spherical structure represents the existence of Al, Fe, Mg, K, Mn and Cl in the product sludge (Akinwekomi et al., 2017, 2020), while the alignment of metals with oxygen denote the formation of metal hydroxides. Overall, the results confirm that the product sludge is the sink for the chemical species contained in the real AMD and CPW and therefore that their passive co-treatment is effective in their removal from these aqueous matrices.

### 3.3.6. Spot analysis

To further substantiate the aforementioned results, spot elemental analysis, by means of SEM-EDX, was also pursued. The spot-morphological characteristics of the product sludge and respective elemental compositions are shown in Fig. 6.

As shown in Fig. 6a, the prominent morphological characteristics of the product sludge were rod-like structures of different lengths and widths, which suggest the formation of gypsum, with few spherical and octagonal-like structures being identified, which suggest the formation of iron-based minerals. The EDX elemental analysis of the product sludge surface (Fig. 6b–g) confirmed the predominance of Ca, S and O in the rod-like structures and of Fe and O in the spherical and octagonal-like structures.

## 3.4. Simulation of the reaction chemistry using PHREEQC

To predict the fate of chemical species after the passive co-treatment of AMD and CPW, the PHREEQC geochemical model was employed. Using the concentration of chemical species in the raw wastewater matrices, as well as those of the co-treated effluent, as inputs, PHREEQC suggested that the chemical species in the raw wastewater matrices mainly existed as di-valent, tri-valent, multi-valents, and oxyanions. However, different complexes were formed during the passive co-treatment, and the respective results, along with the corresponding SI values, are reported in Table 4.

The mineral phases that are more likely to precipitate, based on each SI value, are summarised in Table 4, where it is shown that chemical species will, most likely, precipitate as hydroxides, carbonates,

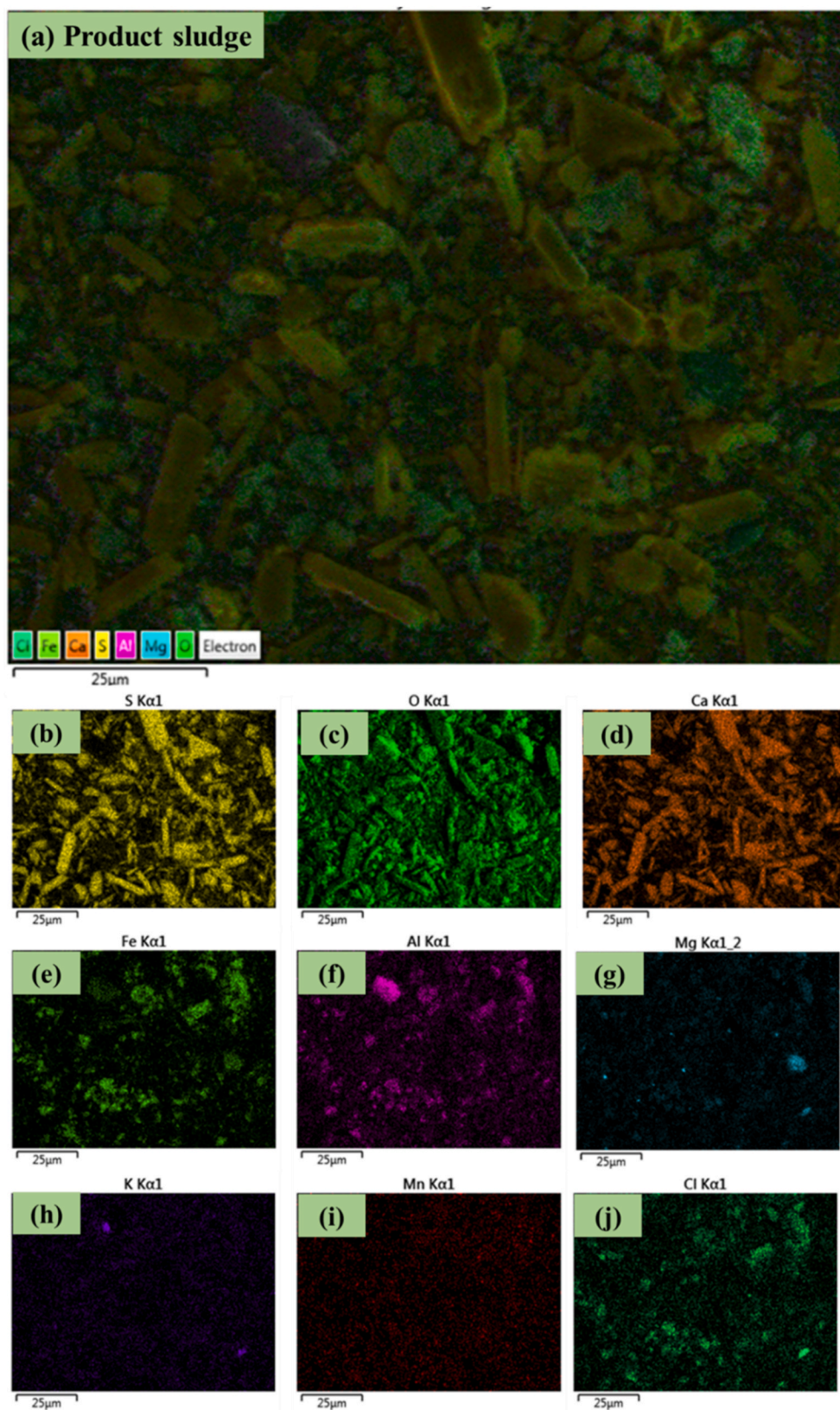


**Fig. 5.** The FE-SEM microstructural image of the product sludge (a) and the elemental mapping images for S (b), O (c), Ca (d), Fe (e), Al (f), Mg (g), K (h), Mn (i), and Cl (j), as determined by EDX.

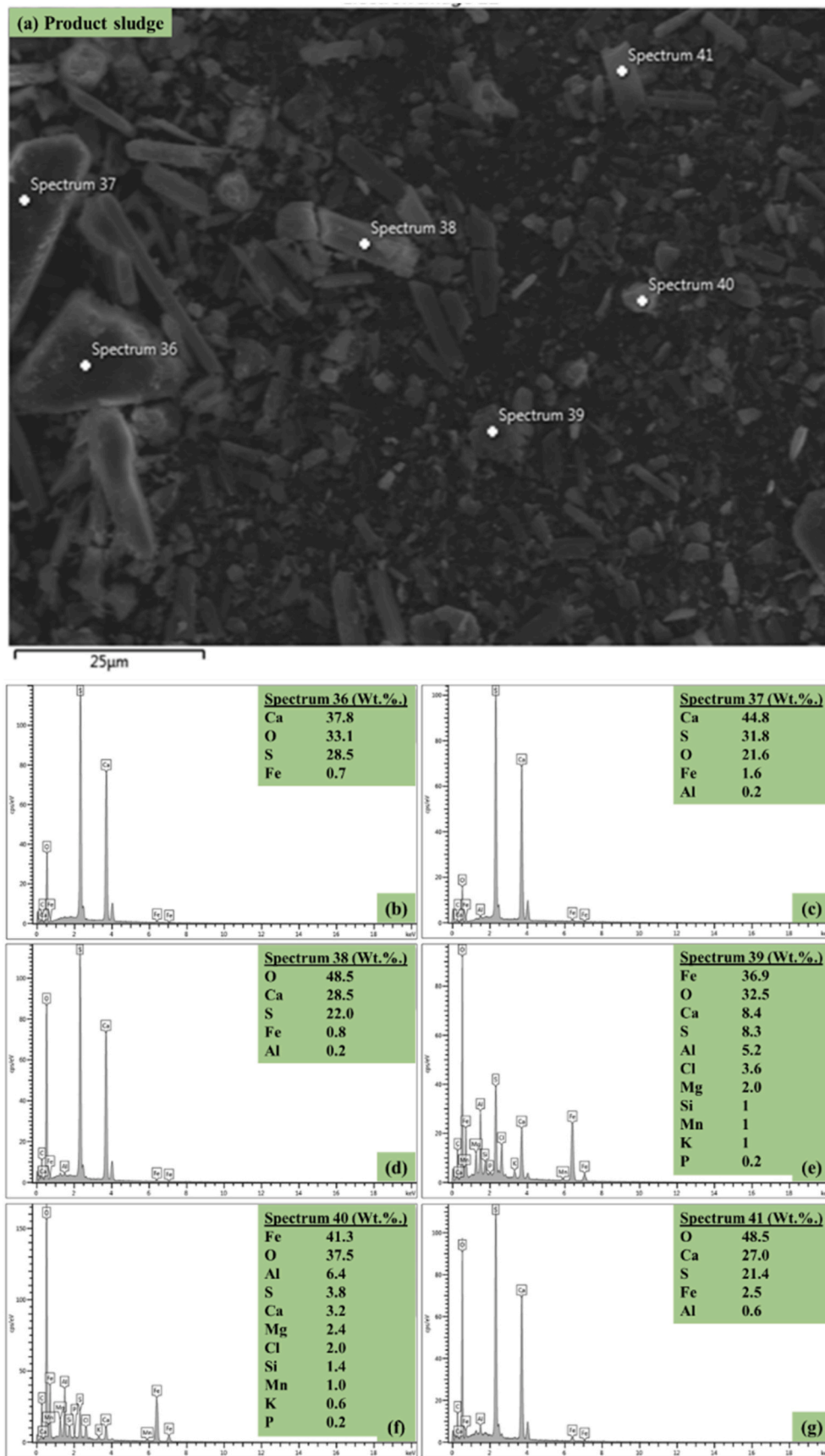


Fig. 6. The SEM-EDX results showing: (a) the spot analysis image of the product sludge, and (b)–(g) the respective spot elemental compositions.

**Table 4**

The chemical names, saturation indexes (SIs), and chemical formulas of the produced minerals from the passive co-treatment of AMD and CPW.

Phase	SI	Chemical formula	Phase	SI	Chemical formula
Anglesite	0.29	PbSO <sub>4</sub>	Huntite	31.03	CaMg <sub>3</sub> (CO <sub>3</sub> ) <sub>4</sub>
Anhydrite	5.3	CaSO <sub>4</sub>	Hydrocerrusite	15.70	Pb(OH) <sub>2</sub> :2PbCO <sub>3</sub>
Aragonite	5.74	CaCO <sub>3</sub>	Langite	9.88	Cu <sub>4</sub> (OH).6SO <sub>4</sub> :H <sub>2</sub> O
AlAsO <sub>4</sub> :2H <sub>2</sub> O	2.29	AlAsO <sub>4</sub> :2H <sub>2</sub> O	Larnakite	4.16	PbO:PbSO <sub>4</sub>
Antlerite	7.32	Cu <sub>3</sub> (OH)4SO <sub>4</sub>	Maghemite	4.53	Fe <sub>2</sub> O <sub>3</sub>
Azurite	16.14	Cu <sub>3</sub> (OH) <sub>2</sub> (CO <sub>3</sub> ) <sub>2</sub>	Magnetite	14.20	Fe <sub>3</sub> O <sub>4</sub>
Basaluminite	1.79	Al <sub>4</sub> (OH)10SO <sub>4</sub>	Malachite	10.52	Cu <sub>2</sub> (OH) <sub>2</sub> CO <sub>3</sub>
Bixbyite	5.47	Mn <sub>2</sub> O <sub>3</sub>	Manganite	2.41	MnOOH
Boehmite	2.59	AlOOH	Mn <sub>3</sub> (AsO <sub>4</sub> ) <sub>2</sub> .8H <sub>2</sub> O	26.84	Mn <sub>3</sub> (AsO <sub>4</sub> ) <sub>2</sub> .8H <sub>2</sub> O
Brochantite	11.70	Cu <sub>4</sub> (OH)6SO <sub>4</sub>	Pb(OH) <sub>2</sub>	2.92	Pb(OH) <sub>2</sub>
Brucite	1.94	Mg(OH) <sub>2</sub>	Pb <sub>3</sub> (AsO <sub>4</sub> ) <sub>2</sub>	21.53	Pb <sub>3</sub> (AsO <sub>4</sub> ) <sub>2</sub>
Bunsenite	0.18	NiO	Pb <sub>4</sub> (OH).6SO <sub>4</sub>	4.61	Pb <sub>4</sub> (OH).6SO <sub>4</sub>
Ca <sub>3</sub> (AsO <sub>4</sub> ) <sub>2</sub> :4H <sub>2</sub> O	14.85	Ca <sub>3</sub> (AsO <sub>4</sub> ) <sub>2</sub> :4H <sub>2</sub> O	Pyrochroite	0.91	Mn(OH) <sub>2</sub>
Calcite	5.88	CaCO <sub>3</sub>	Rhodochrosite	9.70	MnCO <sub>3</sub>
Cerrusite	6.86	PbCO <sub>3</sub>	Scoridite	0.79	FeAsO <sub>4</sub> :2H <sub>2</sub> O
Cupricferrite	16.85	CuFe <sub>2</sub> O <sub>4</sub>	Smithsonite	3.22	ZnCO <sub>3</sub>
Cuprousferrite	17.46	CuFeO <sub>2</sub>	Zn <sub>2</sub> (OH).2SO <sub>4</sub>	3.22	Zn <sub>2</sub> (OH).2SO <sub>4</sub>
Diaspora	4.30	AlOOH	Zn <sub>3</sub> (AsO <sub>4</sub> ) <sub>2</sub> .2.5H <sub>2</sub> O	23.55	Zn <sub>3</sub> (AsO <sub>4</sub> ) <sub>2</sub> .2.5H <sub>2</sub> O
Dolomite	15.90	CaMg(CO <sub>3</sub> ) <sub>2</sub>	Zn(OH) <sub>2</sub>	2.91	Zn(OH) <sub>2</sub>
Gibbsite	2.69	Al(OH) <sub>3</sub>	ZnCO <sub>3</sub> :H <sub>2</sub> O	7.06	ZnCO <sub>3</sub> :H <sub>2</sub> O
Goethite	6.27	FeOOH	Crocoite	0.95	PbCrO <sub>4</sub>
Hausmannite	11.34	Mn <sub>3</sub> O <sub>4</sub>	Chromite	17.30	FeCr <sub>2</sub> O <sub>4</sub>
Hematite	14.92	Fe <sub>2</sub> O <sub>3</sub>	CuCr <sub>2</sub> O <sub>4</sub>	10.09	CuCr <sub>2</sub> O <sub>4</sub>

oxyhydrosulphates, metal oxides, metal sulphates, metals hydro-sulphates, and other sulphates. In particular, sulfate is predicted to be removed as gypsum, metal hydrosulfate, and oxyhydrosulphates; Fe and Al as iron (oxy)-hydroxides and aluminium (oxy)-hydroxides including oxyhydrosulphates; Mg as brucite, magnesite, and dolomite; Ca as gypsum, dolomite, and calcite, including other metalloids based complexes; Pb, Cu, Zn, and Ni as metals hydroxides, metals oxides, metals sulphates, and other complexes; while Mn as carbonates, hydroxides, oxide, and other miscellaneous complexes. Key mechanisms that influence the removal of contaminants were dilution, complexation, (co) adsorption, crystallization, and (co)precipitation. These estimates corroborate the XRD results and also shed light on possible amorphous phases that are most likely to be formed (Table 4). Overall, the predicted mineral phases are congruent to what has been reported in literature (Winfrey et al., 2010; Strosnider et al., 2011, 2013b) and are also complementary to the aforementioned results. Furthermore, it appears that different minerals are found in the product sludge, and this might present a novel avenue for minerals recovery and synthesis. However, toxic elements such as heavy metals are also included in the product sludge, highlighting that its toxicity should also be considered not only when beneficiation opportunities are examined but also when handling and managing the sludge.

#### 4. Conclusions and recommendations

The passive co-treatment, i.e., no energy or resources/reagents are consumed during mixing, of calcium phosphate synthesis wastewater (CPW) and acid mine drainage (AMD) was examined. Results suggest that the passive co-treatment of AMD and CPW is feasible and realistic. The efficacy of the process is primarily governed by underlying chemical reactions between the different contaminants contained in each wastewater matrix, mainly leading to the formation of (hydr)oxides and different complexes which then (co)precipitate. Specifically, the key mechanisms that governed the removal of contaminants were dilution, complexation, (co)adsorption, crystallization, and (co)precipitation. Furthermore, low AMD:CPW ratios, i.e., AMD is diluted into higher CPW volumes, were found to improve the passive co-treatment efficiency, with the optimal AMD:CPW ratio being 1:9. The effective contact time was 12 h of passive reaction with exposure to atmospheric air and ambient temperature and pH. Advanced analytical techniques, including FTIR and FE-SEM/FIB/EDX, shed light on the fate of the chemical species after the passive co-treatment process. Specifically,

contaminants from both wastewater matrices were successfully removed and (co)precipitated in the produced sludge. The sludge microstructural properties included nano rod-like structures and to a lesser extent spherical- and octagonal-like structures homogeneously distributed across its surface. Furthermore, the PHREEQC model suggested that chemical species initially existed as oxyanions, mono-, di-, and tri-valent ions and other complexes and (co)precipitated as hydroxides, carbonates, oxyhydrosulphates, metal oxides, metal sulphates, metals hydro-sulphates, and other sulphates.

Overall, the passive co-treatment of different wastewater matrices, in this case AMD and CPW, appears to hold great promise for their pre-treatment and could lead to their sustainable management, particularly in the developing world setting where infrastructure and resources are limited. It can also safeguard the environment and curtail ecological impacts associated with the discharge of untreated effluents from different industrial processes. Given that phosphorus recovery systems are gaining increasing attention, large amounts of phosphorus-depleted wastewaters are expected to be generated and therefore their passive co-treatment with AMD can present certain advantages for the sustainable management of both wastewater matrices. Opportunities for the beneficiation of the produced sludge and water reclamation might also arise, thus contributing, among others, to United Nations Sustainable Development Goal (SDG) 6 - Water and Sanitation. Finally, the scaling up of the proposed passive co-treatment method could also be direct since this could possibly take place in existing or new waste stabilization ponds. Lastly, future prospects should include the study of the toxicity of the product sludge, as well as its beneficiation, along with the possibility of water reclamation from the co-treated effluent.

#### Credit author statement

**V Masindi** (Conceptualization, Validation, Formal analysis, Investigation, Resources, Data Curation, Writing - Original Draft, Writing - Review & Editing, Visualization, Funding acquisition, and Project administration); **A Shabalala** (Conceptualization, Validation, Formal analysis, Investigation, Data Curation, and Writing - Review & Editing, Visualization), and **S Foteinis** (Conceptualization, Validation, Formal analysis, Investigation, Data Curation, and Writing - Review & Editing, Visualization).

## Declaration of competing interest

The authors declare that they have no known competing financial interests or personal relationships that could have appeared to influence the work reported in this paper.

## Data availability

Data will be made available on request.

## Acknowledgement

The authors would like to thank Magalies Water, the University of South Africa, and University of Mpumalanga for supporting this project. Furthermore, the staff from the municipal wastewater treatment house and mining houses are duly acknowledged for their support with sampling and access to the corresponding facilities. Finally, we would also like to thank the technicians who assisted with the analysis and are employed in the corresponding labs.

## References

- Agboola, O., 2019. The role of membrane technology in acid mine water treatment: a review. *Kor. J. Chem. Eng.* 36, 1389–1400.
- Akinwekomi, V., Maree, J.P., Masindi, V., Zvinowanda, C., Osman, M.S., Foteinis, S., Mpenyana-Monyatsi, L., Chatzisyseon, E., 2020. Beneficiation of acid mine drainage (AMD): a viable option for the synthesis of goethite, hematite, magnetite, and gypsum – gearing towards a circular economy concept. *Miner. Eng.* 148, 106204.
- Akinwekomi, V., Maree, J.P., Zvinowanda, C., Masindi, V., 2017. Synthesis of magnetite from iron-rich mine water using sodium carbonate. *J. Environ. Chem. Eng.* 5, 2699–2707.
- Amos, R.T., Blowes, D.W., Bailey, B.L., Sego, D.C., Smith, L., Ritchie, A.I.M., 2015. Waste-rock hydrogeology and geochemistry. *Appl. Geochem.* 57, 140–156.
- Cheng, S., Jang, J.-H., Dempsey, B.A., Logan, B.E., 2011. Efficient recovery of nano-sized iron oxide particles from synthetic acid-mine drainage (AMD) water using fuel cell technologies. *Water Res.* 45, 303–307.
- Egle, L., Rechberger, H., Krampe, J., Zessner, M., 2016. Phosphorus recovery from municipal wastewater: an integrated comparative technological, environmental and economic assessment of P recovery technologies. *Sci. Total Environ.* 571, 522–542.
- Hughes, T.A., Gray, N.F., 2013. Co-treatment of acid mine drainage with municipal wastewater: performance evaluation. *Environ. Sci. Pollut. Control Ser.* 20, 7863–7877.
- Ighalo, J.O., Kurniawan, S.B., Iwuozor, K.O., Aniagor, C.O., Ajala, O.J., Oba, S.N., Iwuchukwu, F.U., Ahmadi, S., Igwegbe, C.A., 2022. A review of treatment technologies for the mitigation of the toxic environmental effects of acid mine drainage (AMD). *Process Saf. Environ. Protect.* 157, 37–58.
- Kefeni, K.K., Msagati, T.A.M., Mamba, B.B., 2017. Acid mine drainage: prevention, treatment options, and resource recovery: a review. *J. Clean. Prod.* 151, 475–493.
- Maha, A.T., 2022. Attenuation of organics contamination in polymers processing effluent using iron-based sludge: process optimization and oxidation mechanism. *Environ. Technol.* 43, 718, 727–2022 v.43 no.5.
- Masindi, V., 2016. A novel technology for neutralizing acidity and attenuating toxic chemical species from acid mine drainage using cryptocrystalline magnesite tailings. *J. Water Proc. Eng.* 10, 67–77.
- Masindi, V., Chatzisyseon, E., Kortidis, I., Foteinis, S., 2018a. Assessing the sustainability of acid mine drainage (AMD) treatment in South Africa. *Sci. Total Environ.* 635, 793–802.
- Masindi, V., Fosso-Kankeu, E., Mamakoa, E., Nkambule, T.T.I., Mamba, B.B., Naushad, M., Pandey, S., 2022a. Emerging remediation potentiality of struvite developed from municipal wastewater for the treatment of acid mine drainage. *Environ. Res.* 210, 112944.
- Masindi, V., Foteinis, S., 2021. Recovery of phosphate from real municipal wastewater and its application for the production of phosphoric acid. *J. Environ. Chem. Eng.* 9, 106625.
- Masindi, V., Foteinis, S., Chatzisyseon, E., 2022b. Co-treatment of acid mine drainage and municipal wastewater effluents: emphasis on the fate and partitioning of chemical contaminants. *J. Hazard Mater.* 421, 126677.
- Masindi, V., Foteinis, S., Renforth, P., Ndiritu, J., Maree, J.P., Tekere, M., Chatzisyseon, E., 2022c. Challenges and avenues for acid mine drainage treatment, beneficiation, and valorisation in circular economy: a review. *Ecol. Eng.* 183, 106740.
- Masindi, V., Gitari, M.W., Tutu, H., De Beer, M., 2014. Neutralization and attenuation of metal species in acid mine drainage and mine leachates using magnesite: a batch experimental approach. In: *An Interdisciplinary Response to Mine Water Challenges*, pp. 640–644.
- Masindi, V., Madzivire, G., Tekere, M., 2018b. Reclamation of water and the synthesis of gypsum and limestone from acid mine drainage treatment process using a combination of pre-treated magnesite nanosheets, lime, and CO<sub>2</sub> bubbling. *Water Res. Indus.* 20, 1–14.
- Masindi, V., Osman, M.S., Mbhele, R.N., Rikhotso, R., 2018c. Fate of pollutants post treatment of acid mine drainage with basic oxygen furnace slag: Validation of experimental results with a geochemical model. *J. Clean. Prod.* 172, 2899–2909.
- Masindi, V., Osman, M.S., Shingwenyana, R., 2019. Valorization of acid mine drainage (AMD): a simplified approach to reclaim drinking water and synthesize valuable minerals – pilot study. *J. Environ. Chem. Eng.* 7, 103082.
- Mavhungu, A., Foteinis, S., Mbaya, R., Masindi, V., Kortidis, I., Mpenyana-Monyatsi, L., Chatzisyseon, E., 2020. Environmental sustainability of municipal wastewater treatment through struvite precipitation: influence of operational parameters. *J. Clean. Prod.*, 124856.
- Muedi, K.L., Brink, H.G., Masindi, V., Maree, J.P., 2021. Effective removal of arsenate from wastewater using aluminium enriched ferric oxide-hydroxide recovered from authentic acid mine drainage. *J. Hazard Mater.* 414, 125491.
- Nguegang, B., Masindi, V., Msagati, Makudali, T.A., Tekere, M., 2022. Effective treatment of acid mine drainage using a combination of MgO-nanoparticles and a series of constructed wetlands planted with *Vetiveria zizanioides*: a hybrid and stepwise approach. *J. Environ. Manag.* 310, 114751.
- Nguegang, B., Masindi, V., Msagati, T.A.M., Tekere, M., 2021. The treatment of acid mine drainage using vertically flowing wetland: insights into the fate of chemical species. *Minerals* 11, 477.
- Nleya, Y., Simate, G.S., Ndlovu, S., 2016. Sustainability assessment of the recovery and utilisation of acid from acid mine drainage. *J. Clean. Prod.* 113, 17–27.
- Nordstrom, D.K., Blowes, D.W., Ptacek, C.J., 2015. Hydrogeochemistry and microbiology of mine drainage: an update. *Appl. Geochem.* 57, 3–16.
- Park, I., Tabelin, C.B., Jeon, S., Li, X., Seno, K., Ito, M., Hiroyoshi, N., 2019. A review of recent strategies for acid mine drainage prevention and mine tailings recycling. *Chemosphere* 219, 588–606.
- Rittmann, B.E., Mayer, B., Westerhoff, P., Edwards, M., 2011. Capturing the lost phosphorus. *Chemosphere* 84, 846–853.
- Shabalala, A., Masindi, V., 2022. Insights into mechanisms governing the passive removal of inorganic contaminants from acid mine drainage using permeable reactive barrier. *J. Environ. Manag.* 321, 115866.
- Shabalala, A.N., Ekolu, S.O., Diop, S., Solomon, F., 2017. Pervious concrete reactive barrier for removal of heavy metals from acid mine drainage – column study. *J. Hazard Mater.* 323, 641–653.
- Simate, G.S., Ndlovu, S., 2014. Acid mine drainage: challenges and opportunities. *J. Environ. Chem. Eng.* 2, 1785–1803.
- Spellman, C.D., Tasker, T.L., Goodwill, J.E., Strosnider, W.H.J., 2020a. Potential implications of acid mine drainage and wastewater cotreatment on solids handling: a review. *J. Environ. Eng.* 146, 03120010.
- Spellman, C.D., Tasker, T.L., Strosnider, W.H.J., Goodwill, J.E., 2020b. Abatement of circumneutral mine drainage by Co-treatment with secondary municipal wastewater. *J. Environ. Manag.* 271, 110982.
- Strosnider, W.H., Winfrey, B.K., Nairn, R.W., 2011. Alkalinity generation in a novel multi-stage high-strength acid mine drainage and municipal wastewater passive Co-treatment system. *Mine Water Environ.* 30, 47–53.
- Strosnider, W.H.J., Nairn, R.W., Peer, R.A.M., Winfrey, B.K., 2013a. Passive co-treatment of Zn-rich acid mine drainage and raw municipal wastewater. *J. Geochem. Explor.* 125, 110–116.
- Strosnider, W.H.J., Winfrey, B.K., Peer, R.A.M., Nairn, R.W., 2013b. Passive co-treatment of acid mine drainage and sewage: anaerobic incubation reveals a regeneration technique and further treatment possibilities. *Ecol. Eng.* 61, 268–273. Part A.
- Tabelin, C.B., Corpuz, R.D., Igarashi, T., Villacorte-Tabelin, M., Alorro, R.D., Yoo, K., Raval, S., Ito, M., Hiroyoshi, N., 2020. Acid mine drainage formation and arsenic mobility under strongly acidic conditions: importance of soluble phases, iron oxyhydroxides/oxides and nature of oxidation layer on pyrite. *J. Hazard Mater.* 399, 122844.
- Tabelin, C.B., Veerawattananun, S., Ito, M., Hiroyoshi, N., Igarashi, T., 2017. Pyrite oxidation in the presence of hematite and alumina: I. Batch leaching experiments and kinetic modeling calculations. *Sci. Total Environ.* 580, 687–698.
- Tony, M.A., Lin, L.-S., 2022a. Iron recovery from acid mine drainage sludge as Fenton source for municipal wastewater treatment. *Int. J. Environ. Anal. Chem.* 102, 1245–1260.
- Tony, M.A., Lin, L.-S., 2022b. Performance of acid mine drainage sludge as an innovative catalytic oxidation source for treating vehicle-washing wastewater. *J. Dispersion Sci. Technol.* 43, 50–60.
- Wei, X., Viadero, R.C., Bhojappa, S., 2008. Phosphorus removal by acid mine drainage sludge from secondary effluents of municipal wastewater treatment plants. *Water Res.* 42, 3275–3284.
- WHO, 2017. Guidelines for Drinking-Water Quality, fourth ed. World Health Organization, Geneva. incorporating first addendum.
- Wilfong, W.C., Ji, T., Duan, Y., Shi, F., Wang, Q., Gray, M.L., 2022. Critical review of functionalized silica sorbent strategies for selective extraction of rare earth elements from acid mine drainage. *J. Hazard Mater.* 424, 127625.
- Winfrey, B.K., Strosnider, W.H., Nairn, R.W., Strevett, K.A., 2010. Highly effective reduction of fecal indicator bacteria counts in an ecologically engineered municipal wastewater and acid mine drainage passive co-treatment system. *Ecol. Eng.* 36, 1620–1626.